Waveform Analysis of Ocular Blood Flow and the Early Detection of Normal Tension Glaucoma

Yukihiro Shiga, Kazuko Omodaka, Hiroshi Kunikata, Morin Ryu, Yu Yokoyama, Satoru Tsuda, Toshifumi Asano, Shigeto Maekawa, Kazuichi Maruyama, and Toru Nakazawa

Department of Ophthalmology, Tohoku University Graduate School of Medicine, Miyagi, Japan

Correspondence: Toru Nakazawa, Department of Ophthalmology, Tohoku University Graduate School of Medicine, 1-1 Seiryo, Aoba, Miyagi 980-8574, Japan; ntoru@oph.med.tohoku.ac.jp.

Submitted: July 28, 2013
Accepted: September 18, 2013

Citation: Shiga Y, Omodaka K, Kunikata H, et al. Waveform analysis of ocular blood flow and the early detection of normal tension glaucoma. *Invest Ophthalmol Vis Sci*. 2013;54:7699–7706. DOI:10.1167/iovs.13-12930

Purpose. To investigate waveform changes in blood flow (BF) in the optic nerve head (ONH) and to evaluate their usefulness in identifying normal tension glaucoma (NTG).

Methods. Sixty-one eyes of 61 patients with NTG and 21 eyes of age-matched healthy control subjects were included in this study. The NTG eyes were divided into the following three groups based on the progression of their visual field defects: mild (mean deviation [MD] greater than −6.0 decibels [dB]), moderate (MD between −6.0 and −12.0 dB), and severe (MD less than −12.0 dB). The ONH BF analysis was performed with laser speckle flowgraphy (LSFG) and included waveform variables such as skew, acceleration time index (ATI), and blowout time.

Results. In the ONH, LSFG skew variables were significantly lower in the NTG eyes than in the control eyes ($P < 0.001$), and ATI was significantly higher ($P < 0.01$), despite similar systemic characteristics in the four groups. The differences were most marked in the mild NTG group. Multiple linear regression analysis showed that MD, average thickness of the circumpapillary retinal nerve fiber layer, and pulse rate were predictive factors for both skew and ATI. A receiver operating characteristic (ROC) curve analysis also revealed that skew (area under the ROC curve, 0.89) and ATI (area under the ROC curve, 0.80) had the greatest power to differentiate normal eyes from eyes with mild NTG.

Conclusions. These results suggest that LSFG measurements of waveform changes in ONH BF can differentiate healthy eyes from eyes with NTG, particularly those with mild NTG.

Keywords: laser speckle flowgraphy, ocular blood flow, waveform analysis, optic nerve head, glaucoma

Glaucoma is the second most common cause of blindness worldwide and affects more than 60 million people.[1] It is characterized by degeneration of the axons in the optic nerve head (ONH) and death of the retinal ganglion cells, corresponding to a structural loss of neural tissue in the ONH and subsequent visual field loss. Although the pathogenesis of glaucoma remains unclear, it is believed to be multifactorial. Increased IOP is the most well-known risk factor for the progression of glaucoma, and IOP reduction is usually effective in slowing the progress of the disease.[2] However, recent epidemiological studies[3–5] have revealed that IOP reduction alone cannot prevent the progression of visual field loss in all patients. Besides increased IOP, a number of studies[6–15] have suggested that both ocular and systemic dysregulation of blood flow (BF) have an important role in the development of glaucoma, especially when IOP is not increased (normal tension glaucoma [NTG]). Thus, an understanding of hemodynamic abnormalities in the ONH may be critical to determine the pathophysiology of NTG because it is a key pressure-independent factor.

Laser speckle flowgraphy (LSFG), a noninvasive technology based on the laser speckle phenomenon, allows the assessment of microcirculation in the ONH, the choroid at the fovea, and the retinal vessels simultaneously.[16] The LSFG technology takes just a few seconds to acquire an image of ocular circulation and has excellent reproducibility.[17] The mean blur rate (MBR), the key parameter of LSFG, represents the relative velocity of erythrocytes.[18,19] It has recently been demonstrated to be highly correlated with results obtained with the microsphere method in nonhuman primates and with the hydrogen gas clearance method in rabbits.[20,21] This makes LSFG a suitable instrument currently available for evaluation of ONH BF.

A new version of LSFG's accompanying software (LSFG Analyzer, version 3.0.43.0; Softcare Ltd., Fukutsu, Japan) has also made it possible to synchronize the images from each cardiac cycle and derive various parameters from the heartbeat waveform. The resulting analysis enables us to quantify changes in MBR in a single heartbeat. In the ONH, blowout time (BOT), one of the derived parameters, can be useful in evaluating early atherosclerotic changes or aging of the microcirculation.[22,23] Furthermore, the LSFG software can measure BF separately in the capillary and large vessel areas of the ONH. The LSFG waveform analysis is thus of great value for assessing the dynamics of ocular BF.

In the field of cardiology, ultrasonographic techniques are also commonly used in clinical practice. Ultrasonography can provide quantitative parameters such as skewness and velocity acceleration through analysis of measured Doppler waveforms and can usefully differentiate healthy patients from those with cardiac disease,[24–26] as well as help evaluate the effects of endothelial dysfunction.[27–30] Doppler velocity profile parameters can thus provide a great deal of information on BF. In the

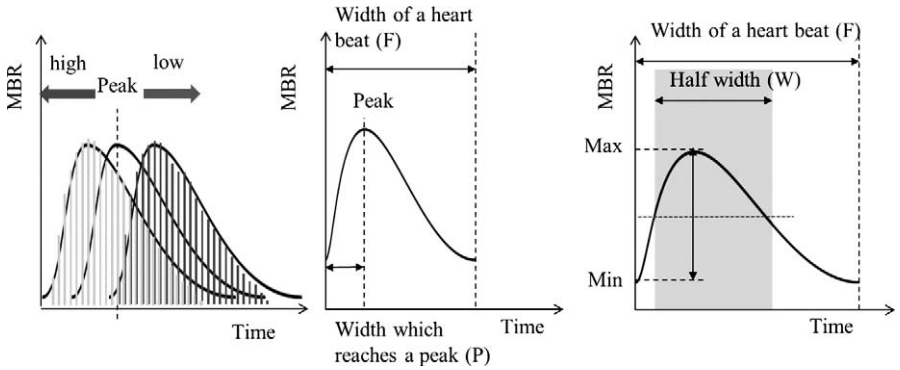

FIGURE 1. Waveform analyses of skew (*left*), ATI (*middle*), and BOT (*right*).

field of ophthalmology, Abegão Pinto et al.[31] used color Doppler imaging (CDI) in a study showing that the pattern of BF velocity in the ophthalmic artery (OA) seems to be altered in patients with glaucoma. This finding motivated us to use LSFG to perform a more detailed investigation of changes in the ONH BF waveform in eyes with glaucoma.

Thus, the purpose of this study was to analyze the ocular waveforms of patients with NTG using LSFG and to compare them with those of healthy subjects. In addition, the study determined which parameters of the analysis could best differentiate between healthy and glaucomatous eyes.

Materials and Methods

Subjects

This case-control study comprised 61 consecutive Japanese patients with NTG and 21 age-matched healthy control subjects who visited Tohoku University Hospital, Miyagi, Japan, between November 2010 and May 2011. Patients with NTG were defined as follows: (1) the presence of glaucomatous optic disc changes and visual field defects according to the Anderson-Pattela classification confirmed in at least two visual field examinations, (2) abnormal circumpapillary retinal nerve fiber layer thinning (cpRNFLT), (3) a normal open angle in a gonioscopic examination, (4) no history of ocular or systemic disease causing optic nerve damage, and (5) no record of IOP greater than 21 mm Hg. The presence of abnormal visual field defects meant that the results of a glaucoma hemifield test were outside normal limits and that a cluster of three or more nonedge points were present, all depressed on the pattern deviation plot at $P < 0.05$ (with one depressed at $P < 0.01$), as well as that the corrected pattern SD was significant at $P < 0.05$. Patients with NTG enrolled in this study also met the following criteria: (1) no ocular laser or incisional surgery in either eye, including cataract surgery; (2) no history of systemic medication use such as antihypertensive, antihyperlipidemic, or hypoglycemic agents; (3) reliable performance in visual field testing (fixation errors < 20%, false positives < 15%, and false negatives < 33%) with the 30-2 Swedish interactive thresholding algorithm standard program of the Humphrey Field Analyzer (Carl Zeiss Meditec, Dublin, CA); and (4) no refractive error less than –6.0 diopters. The eyes with NTG were divided into the following three groups based on the progression of their visual field defects: mild (mean deviation [MD] greater than –6.0 decibels [dB]), moderate (MD between –6.0 and –12.0 dB), and severe (MD less than –12.0 dB). Healthy subjects included in this study all had baseline IOP in both eyes below 21 mm Hg and normal findings in a slitlamp and funduscopic examination. Healthy subjects were excluded if they manifested abnormal cpRNFLT or visual field defects, had a history of ocular or general disorders, were using systemic or topical medication, or smoked regularly. The procedures in this study followed the tenets of the Declaration of Helsinki and were approved by the institutional review board of the Tohoku University Graduate School of Medicine.

Measurement of Clinical Parameters

The IOP was measured using Goldmann applanation tonometry. The visual field was measured with the 30-2 program of the Humphrey Field Analyzer (Carl Zeiss Meditec), and cpRNFLT was assessed with 3D OCT-2000 (version 8.00; Topcon, Inc., Tokyo, Japan). Both systemic blood pressure (BP) and pulse rate (PR) were measured in the left brachial artery at the height of the heart with an automated BP monitor (HEM-759E; Omron Corporation, Kyoto, Japan) with the subject in a sitting position. The BP amplitude was calculated from systolic BP (SBP) and diastolic BP (DBP) according to the following formula: BP Amplitude = SBP − DBP. The mean arterial pressure (MAP) was calculated according to the following formula: MAP = DBP + 0.42 (SBP − DBP).[32–34] Ocular perfusion pressure (OPP) was calculated according to the following formula: OPP = 2/3 MAP − IOP.[35]

Determination of Waveform Analysis Parameters in the ONH Using LSFG

The principles of LSFG (Softcare Ltd.) have been described in detail previously.[36,37] Briefly, this instrument consists of a fundus camera equipped with a diode laser (wavelength, 830 nm) and an ordinary charge-coupled device camera (750 [width] × 360 [height] pixels). The MBR, the relative velocity of BF, is determined using the pattern of speckle contrast produced by the interference of a laser scattered by blood cells moving in the ocular fundus.[18] The MBR images are acquired continuously at the rate of 30 frames per second over a 4-second period. The accompanying analysis software then synchronizes all captured MBR images with each cardiac cycle, and the averaged MBR of a heartbeat is displayed as a heartbeat map. The software next divides the MBR in the ONH into the large vessel and capillary areas automatically. In this study, we examined waveform changes only in the capillary area of the ONH. The last step of the analysis was to calculate the skew, acceleration time index (ATI), and BOT (Fig. 1) of the MBR waveform as it changed over the course of a single heartbeat. Skew is a histogram of the MBR distribution of a heartbeat (Fig. 1, left) and varies with the bias of the BF velocity profile. If the distribution of the waveform is leftward, skew is higher, and if

Table 1. Baseline Clinical Characteristics of the Four Study Groups

Variable	Normal, $n = 21$	NTG, $n = 61$			P Value
		Mild, $n = 21$	Moderate, $n = 20$	Severe, $n = 20$	
Age, y	57 (53.0–62.0)	59 (53.0–66.5)	58.5 (52.0–63.0)	62 (57.3–65.0)	NS*
Ratio of men to women	12:9	8:13	12:8	13:7	NS†
Refractive error, diopters	−1.1 (−3.2–0.0)	−2.0 (−3.5 to −0.2)	−0.9 (−4.1–0.4)	−3.1 (−4.0 to −2.0)	NS*
IOP, mm Hg	12.3 (11.1–14.8)	15.0 (10.5–16.0)	13.0 (11.3–14.0)	14.5 (13.3–17.5)	NS*
MD, dB	0.8 (0.1–1.3)	−3.7 (−4.8 to −2.4)	−8.3 (−9.8 to −7.5)	−19.7 (−22.9 to −15.3)	<0.001*
cpRNFLT, μm	119.3 (111.3–126.0)	74.8 (66.5–90.8)	67.0 (60.0–76.2)	48.9 (45.5–61.3)	<0.001*
BP, mm Hg					
SBP	121.0 (113.5–134.5)	123.0 (117.5–139.0)	123.5 (114.0–141.5)	124.0 (111.8–141.8)	NS*
DBP	73.0 (68.0–80.0)	80.0 (64.5–87.0)	74.0 (67.0–90.3)	70.0 (67.0–85.0)	NS*
BP amplitude, mm Hg	48.0 (42.5–56.5)	47.0 (43.5–57.0)	46.5 (40.3–53.0)	46.5 (43.0–55.5)	NS*
MAP, mm Hg	93.6 (87.4–100.3)	98.1 (86.6–107.8)	93.9 (87.0–113.2)	92.5 (85.8–107.0)	NS*
OPP, mm Hg	50.3 (47.2–53.3)	51.6 (47.4–55.7)	53.1 (48.7–57.5)	50.1 (47.1–53.0)	NS*
PR, beats/min	71.0 (65.5–78.0)	79.0 (71.5–87.5)	73.0 (62.0–83.0)	74.5 (65.3–86.8)	NS*
Topical antiglaucoma medication					
Prostaglandin analogue	...	16 (76.2)	15 (75.0)	19 (95.0)	NS†
β-antagonist	...	9 (42.9)	10 (47.6)	14 (70.0)	
Carbonic anhydrase inhibitor	...	5 (23.8)	9 (45.0)	13 (65.0)	
α-1-antagonist	...	1 (4.8)	4 (20.0)	7 (35.0)	
Antiglaucoma medications, n (%)					
4	...	1 (4.8)	2 (10.0)	6 (30.0)	NS†
3	...	2 (9.5)	7 (35.0)	5 (25.0)	
2	...	7 (33.3)	2 (10.0)	5 (25.0)	
1	...	7 (33.3)	5 (25.0)	4 (20.0)	
0	...	4 (19.0)	4 (20.0)	0	

Unless otherwise indicated, data are expressed as the median (interquartile range). Differences were considered significant at $P < 0.05$. NS, not significant.

* Differences between groups were assessed with Kruskal-Wallis test, followed by Steel-Dwass test.

† McNemar test was used for the frequency data of sex and topical antiglaucoma medication use.

the distribution is rightward, skew is lower. A value of zero indicates a symmetrical profile. Additionally, the value of skew decreases as the slope of the waveform after the peak becomes more gradual, indicating a flattened drop-off in BF after the peak. Thus, even if the position of the peak is the same, the value of skew will be smaller if the slope is more gradual. Skew is calculated as follows:

$$Skew = C \cdot \sum_{k=1}^{N} \left\{ \left(\frac{k - Ave}{Stdev} \right)^3 \cdot p(k) \right\}$$

$$Ave = \sum_{k=1}^{N} \{k \cdot p(k)\}$$

$$Stdev = \sqrt{\sum_{k=1}^{N} \{(k - Ave)^2 \cdot p(k)\}}$$

The N indicates the number of frames, and the changing MBR waveform of a heartbeat is divided into N frames. The k represents the average of MBR in the k frame, and C is the constant of proportion. The *Ave* indicates average of normalized MBR waveform of a heartbeat. The *Stdev* represents the standard deviation of normalized MBR waveform of a heartbeat. The p (k) indicates the probability density function in the k frame. The ATI shows the duration to reach the peak of MBR, and the value is calculated according to the following formula: ATI = (Duration to Reach Peak/Duration of a Heartbeat) ×100 (Fig. 1, middle). The BOT was calculated according to the following formula: BOT = (Half Width/Width of a Heartbeat) ×100 (Fig. 1, left).[22,23]

Reproducibility Assessment of LSFG Waveform Analysis Parameters

The intrasession reproducibility of LSFG waveform variables was assessed. The coefficient of variation (COV) was calculated for LSFG measurements obtained with LSFG in three continuous examinations on the same day.

Testing Protocol

On the day of the test, after a slitlamp examination, 0.4% tropicamide (Mydrin M; Santen Pharmaceutical Co., Ltd., Osaka, Japan) was used to dilate the pupil. All subjects received a funduscopic examination, cpRNFLT was measured with 3D OCT-2000 (version 8.00; Topcon, Inc.), and IOP was measured with Goldmann applanation tonometry. The patients rested in a sitting position for 10 minutes in a dark room before the examination. The SBP, DBP, and PR were recorded, and ONH circulation was measured with LSFG three times. Averaged variables were used for the statistical analysis, which used one randomly selected eye from each of the subjects. The LSFG measurement was performed by neutral observers unaware of the clinical status of the subjects. Ongoing medical treatment, including IOP-lowering topical medication in the patients with NTG, was not interrupted before the examination.

Table 2. Waveform Analysis Results of ONH BF in the Four Study Groups

Variable	Normal, $n = 21$	NTG, $n = 61$			P Value
		Mild, $n = 21$	Moderate, $n = 20$	Severe, $n = 20$	
Skew, AU	13.1 (12.3–14.0)	10.4 (9.9–11.6)	12.1 (10.7–12.8)	11.9 (10.6–12.8)	<0.001
ATI, AU	29.6 (27.5–31.9)	33.5 (31.4–36.0)	32.6 (29.3–35.4)	31.0 (29.4–33.1)	<0.01
BOT, AU	48.2 (44.0–50.2)	49.8 (47.5–53.1)	49.4 (45.6–52.1)	48.8 (44.6–54.0)	NS

Data are expressed as the median (interquartile range). Differences were considered significant at $P < 0.05$. Differences between groups were assessed with Kruskal-Wallis test, followed by Steel-Dwass test. NS, not significant.

Statistical Analysis

All data are expressed as the median (interquartile range). Kruskal-Wallis test, followed by Steel-Dwass test, was used to analyze the significance of differences in the four groups. McNemar test was used for frequency data on sex and the number of topical antiglaucoma medications. Spearman rank correlation test was used to evaluate single correlations between variables. Multiple linear regression analysis was performed to determine independent variables affecting the waveform parameters, MD, and cpRNFLT. A receiver operating characteristic (ROC) curve for the waveform parameters was plotted to determine the optimum cutoff point, and the area under the ROC curve (AUC) was used to determine the discrimination power between normal and NTG eyes. All statistical analyses were performed with JMP software (Pro version 10.0.2; SAS Institute Japan, Inc., Tokyo, Japan). The significance level was set at $P < 0.05$.

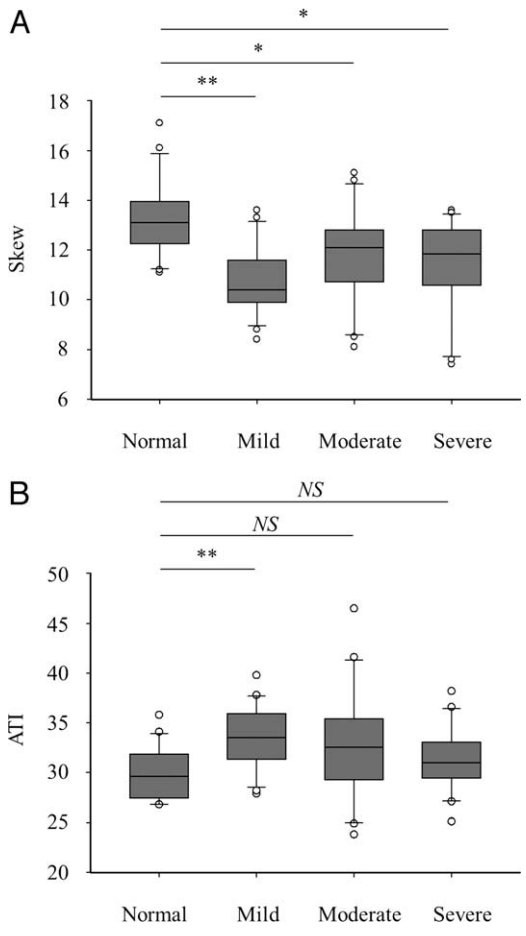

Figure 2. Box plots of skew (**A**) and ATI (**B**) showing differences in the waveform variables in the four study groups. The *bottom* and *top* of the *boxes* represent the first and third quartiles, respectively, while the *lines* inside the boxes indicate the second quartile. The *ends of the whiskers* represent the 10th and 90th percentiles. Outlying values are included as *small circles*. The *asterisks* indicate statistically significant differences compared with normal eyes (Kruskal-Wallis test, followed by Steel-Dwass test; *$P < 0.05$, **$P < 0.01$).

Results

Baseline Clinical Characteristics

Table 1 summarizes the baseline clinical characteristics of the four study groups and their comparative P values. Kruskal-Wallis test and McNemar test revealed no significant differences among the four groups in age, sex distribution, refractive error, IOP, cardiovascular variables (SBP, DBP, BP amplitude, MAP, OPP, and PR), frequency of topical medication use, or the number of topical antiglaucoma medications (range, $P = 0.10$ to $P = 0.89$). The MD and cpRNFLT among the patients with glaucoma were significantly different from those among the controls ($P < 0.001$ for both).

Reproducibility of LSFG Waveform Analysis Parameters

The reproducibility of each LSFG waveform analysis parameter in the capillary area of the ONH was similar. The COVs were 8.70% ± 4.26% for skew, 6.55% ± 5.57% for ATI, and 5.40% ± 5.57% for BOT.

LSFG Waveform Analysis Parameters

Table 2 gives an overview of the LSFG data from the capillary area of the ONH in the four study groups. Skew was significantly lower in the NTG eyes than in the controls ($P < 0.001$), while ATI was significantly higher ($P < 0.01$). Skew was significantly lower in each stage of NTG among healthy controls ($P < 0.001$ for normal versus mild, $P = 0.03$ for normal versus moderate, and $P = 0.01$ for normal versus severe) (Fig. 2A). On the other hand, while ATI was significantly higher among the patients with mild NTG than among the controls ($P < 0.01$), there was no significant difference between the moderate ($P = 0.15$) and severe ($P = 0.38$) NTG eyes and the controls (Fig. 2B). There was no significant difference in BOT among the four study groups ($P = 0.32$). The MBRs in the capillary area of the ONH in each group were 14.12 ± 1.47 arbitrary units (AU) for normal, 11.54 ± 2.84 AU for mild, 10.19 ± 1.65 AU for moderate, and 9.16 ± 2.62 AU for severe.

Relationship Between LSFG Waveform Variables and Other Variables

Single regression analysis showed that skew was significantly correlated with refractive error ($r = 0.28$, $P = 0.01$), DBP ($r = -0.22$, $P = 0.04$), BP amplitude ($r = 0.34$, $P < 0.01$), PR ($r =$

Table 3. Multiple Regression Analysis of Independent Variables Affecting Skew

Dependent Variable	β	*P* Value
Age	0.07	0.47
IOP	0.02	0.81
MD	−0.34	0.02
cpRNFLT	0.67	<0.001
PR	−0.31	<0.01
BP amplitude	0.28	<0.01

β is the standardized coefficient. Differences were considered significant at $P < 0.05$.

–0.34, $P < 0.01$), MD ($r = 0.28$, $P = 0.01$), and cpRNFLT ($r = 0.41$, $P < 0.01$). The ATI was significantly correlated with DBP ($r = 0.23$, $P = 0.04$), MAP ($r = 0.22$, $P = 0.04$), OPP ($r = 0.26$, $P = 0.02$), PR ($r = 0.39$, $P < 0.01$), and cpRNFLT ($r = –0.31$, $P < 0.01$). The BOT was significantly correlated with age ($r = –0.31$, $P < 0.01$), SBP ($r = –0.28$, $P = 0.01$), and BP amplitude ($r = –0.32$, $P < 0.01$). Multiple linear regression analysis showed that MD ($\beta = –0.34$, $P = 0.02$), cpRNFLT ($\beta = 0.67$, $P < 0.001$), PR ($\beta = –0.31$, $P < 0.01$), and BP amplitude ($\beta = 0.28$, $P < 0.01$) were predictors of skew (Table 3). Additionally, MD ($\beta = 0.38$, $P = 0.02$), cpRNFLT ($\beta = –0.55$, $P < 0.001$), and PR ($\beta = 0.36$, $P < 0.01$) were predictors of ATI (Table 4).

Power of the LSFG Waveform Variables to Differentiate Between Normal Eyes and NTG Eyes

Table 5 compares the AUC analyses among the four study groups. Notably, the values for skew (AUC, 0.89) and ATI (AUC, 0.80) showed greater power to differentiate between normal eyes and eyes with mild NTG than eyes with severe NTG.

The ROC curves for skew and ATI showed the following: (1) the cutoff point for skew was 12.5, (2) the cutoff point for ATI was 31.3 for the controls and all patients with NTG, and (3) the cutoff point for skew was 12.6 and the cutoff point for ATI was 32.0 for the controls and the patients with mild NTG. Figure 3 shows a representative waveform for the ONH capillary area in the healthy controls and the patients with mild NTG.

Discussion

We set out to determine whether LSFG measurements of BF waveform changes in the ONH could have a useful role in the diagnosis of NTG. We found that skew was significantly lower and ATI was significantly higher in the ONH of eyes with mild NTG than in healthy controls, although we found no significant difference in systemic characteristics between the patients with NTG in our study and healthy controls. Furthermore, multiple linear regression analysis showed that MD, cpRNFLT, and PR were predictors of these significantly altered skew and ATI values. The ROC curve analysis further revealed that altered skew and ATI values were good indicators of eyes with mild NTG. This suggests that LSFG-derived measurements of skew and ATI may have value as new noninvasive and objective biomarkers of mild NTG.

Table 4. Multiple Regression Analysis of Independent Variables Affecting ATI

Dependent Variable	β	*P* Value
Age	0.15	0.14
IOP	−0.13	0.22
MD	0.38	0.02
cpRNFLT	−0.55	<0.001
PR	0.36	<0.01
BP amplitude	−0.04	0.68

β is the standardized coefficient. Differences were considered significant at $P < 0.05$.

Table 5. Waveform Variables AUC Comparison in Normal Eyes and NTG Eyes

Variable	Normal vs. All NTG	Normal vs. Mild NTG
Skew	0.81 (0.68–0.89) $P < 0.001$	0.89 (0.74–0.95) $P < 0.001$
ATI	0.72 (0.58–0.82) $P = 0.02$	0.80 (0.64–0.91) $P < 0.01$

Data are expressed as the AUC (95% confidence interval). Differences were considered significant at $P < 0.05$.

Our study's main investigative tool was LSFG, which we used to measure the BF waveform of the ONH in patients with NTG. We then analyzed a number of parameters of the resulting waveform. We found tendencies toward a delay in the peak of the waveform, a flattened waveform, and lowered MBR amplitude of the heartbeat. Significant increases in ATI and significant decreases in skew were associated with these waveform changes in NTG, particularly in mild cases. These findings complement studies[29,30,38,39] in the field of cardiology demonstrating that velocity acceleration can affect endothelial cell function and that acceleration time, a measure of the time taken to reach peak BF, shows a delay correlated with the severity of ventricular stenosis. Other studies have demonstrated that an initial burst of nitric oxide (NO) is dependent on velocity acceleration[40,41] and that velocity acceleration decreases in cardiac ischemic diseases, with age, and with increased vascular resistance.[27,28,42,43] In the ONH too, evidence has shown that NO and endothelin may be key regulators of BF.[44] The ONH BF also changes in glaucoma, and although the cause remains unclear, the disease has been reported to be associated with an imbalance between NO and endothelin, a characteristic of endothelial dysfunction.[45] In addition, studies[6,46] using CDI to examine patients with NTG have revealed increased vascular resistance in the OA. Most recently, Abegão Pinto et al.[31] demonstrated using CDI that patients with primary open-angle glaucoma (POAG) have lower early systolic acceleration in the OA compared with healthy subjects.[31] Thus, our findings on the increase in ATI and the decrease in skew in mild NTG may indicate that endothelial dysfunction or increased vascular resistance has a role.

We hypothesize that waveform changes in the mild stages of glaucoma may be caused by a collapse of the ONH's BF

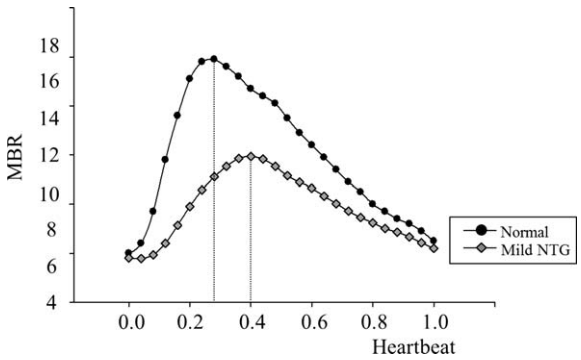

Figure 3. Representative LSFG waveforms of ONH BF in normal eyes and eyes with mild NTG. The *dots on the lines* indicate the MBR in the capillary area at each measured time point. The *vertical lines* show the delay in peak MBR in the mild NTG eyes compared with the normal eyes.

autoregulation mechanism, resulting in endothelial dysfunction and tissue remodeling. It is already well known that extensive remodeling of the extracellular matrix (ECM) is associated with optic neuropathy in glaucoma.[47] There are also studies[48,49] demonstrating that eyes with glaucoma show accelerated aging and that age-related increases in laminar ECM stiffening can alter nutrient diffusion from the laminar capillaries into the adjacent axons. Our findings are reinforced by studies[25,26,50] showing that skewness, a Doppler waveform parameter, indicates velocity distribution and can differentiate healthy patients from those with cardiac disease. In addition, it has been reported that not only BF but also cardiac anatomical structures such as localized basal septal hypertrophy can affect skewness in the ventricular outflow tract.[26] Taken together, these findings suggest that extensive ONH remodeling of the ECM may have affected the decreased skew among patients with mild NTG in this study.

Multiple linear regression analysis showed that cardiovascular parameters were predictors of ATI (PR) and skew (BP amplitude and PR), indicating that these LSFG-derived values may reflect systemic circulation. We did not find significant differences in BOT in any of the NTG or control groups in our study. Because BOT represents the full duration of the waveform at half its maximum value, the variable can rise with the progression of glaucomatous change and subsequent flattening of the waveform. Although BOT, one of the waveform parameters, has been shown to be strongly correlated with age[22,23] and the occurrence of glaucoma has also been reported to be associated with age,[51,52] we did not observe any relationship between BOT and the severity of NTG. It remains unclear why this was so, but the explanation may lie in the fact that there were no differences in age, systemic BP, or PR among the NTG or control groups included in our study. We therefore consider that the significant changes in ATI and skew that we observed are phenomena specific to mild NTG.

We believe that the ability to detect mild NTG with a noninvasive examination such as LSFG could become a useful part of annual health examinations. Mild NTG is an often asymptomatic stage of the disease, and there may be a very large part of the population that is currently undiagnosed. Our AUC analysis showed that the waveform values of skew and ATI had the most potential to be useful in the diagnosis of mild NTG. We also found that LSFG waveform variables had a good level of reproducibility, reinforcing our previous findings on the reproducibility of MBR-derived values.[17] Although it remains unclear why early glaucomatous changes in ATI and skew disappeared as NTG progressed to the moderate and severe stages, it may be that the baseline of a single beat became depressed and the waveform became extremely flattened as NTG progressed beyond the moderate level. Skew also decreased not only as the peak shifted rightward but also as the descending speed after the peak decreased. It has been reported that there are significant decreases in the numbers of ONH capillaries and axons in eyes with POAG.[53] Although the present study was limited to NTG and did not include patients with POAG, a similar reduction would lend support to our finding that the waveform became flattened as NTG progressed. This may also be associated with our finding that LSFG waveform variables had the strongest differentiating power between normal eyes and those with mild NTG.

The present study was limited by its retrospective and cross-sectional design, and the measurements were done in the patients with glaucoma without discontinuing their current antiglaucoma medications. Previous clinical studies[54–58] had reported that a number of topical prostaglandin analogues (PG; e.g., latanoprost, unoprostone, and tafluprost) and combined topical therapy with timolol (a β-antagonist) and dorzolamide (a carbonic anhydrase inhibitor) caused a significant increase in ONH BF. Other studies[59,60] showed no effects of topical antiglaucoma medications on ONH BF. Thus, any effects of topical antiglaucoma medications on ONH BF are controversial. In this study, there were no significant differences in the frequency of topical medication use or the number of topical antiglaucoma medications in the three stages of NTG. Notably, we found that there was no effect on skew (10.8 ± 1.2 AU for the PG group and 10.9 ± 1.6 AU for the non-PG group [$P = 0.85$]) or ATI (33.4 ± 3.4 AU for the PG group and 33.5 ± 1.3 AU for the non-PG group [$P = 0.93$]) in patients with mild NTG either taking PG or not taking it. Thus, the subjects' use of topical medication may have had an impact on waveform changes in the ONH. There is a need for validation of our results with a prospective study that includes a larger number of subjects without treatment for glaucoma. It would also be useful to obtain a better understanding of the mechanism of waveform change in NTG and more complete knowledge of whether this change is comparable to that in POAG and preperimetric glaucoma.

In conclusion, LSFG measurement of the ONH revealed decreased skew and increased ATI in eyes with mild NTG. Multiple linear regression analysis showed that MD and cpRNFLT contributed independently to both skew and ATI. The ROC curve analysis revealed that skew and ATI could differentiate healthy eyes from those with mild NTG. These results suggest that LSFG values for skew and ATI may be new noninvasive and objective biomarkers of NTG and may become a useful part of the clinical decision-making process in early glaucoma.

Acknowledgments

The authors thank Masayuki Yasuda, Naoko Aizawa, Ai Shimizu, Masayoshi Yukita, and Takehiro Hariya for valuable comments and thank Tim Hilts for reviewing the manuscript.

Disclosure: **Y. Shiga**, None; **K. Omodaka**, None; **H. Kunikata**, None; **M. Ryu**, None; **Y. Yokoyama**, None; **S. Tsuda**, None; **T. Asano**, None; **S. Maekawa**, None; **K. Maruyama**, None; **T. Nakazawa**, None

References

1. Quigley HA, Broman AT. The number of people with glaucoma worldwide in 2010 and 2020. *Br J Ophthalmol*. 2006;90:262–267.
2. Kass MA, Heuer DK, Higginbotham EJ, et al. The Ocular Hypertension Treatment Study: a randomized trial determines that topical ocular hypotensive medication delays or prevents the onset of primary open-angle glaucoma. *Arch Ophthalmol*. 2002;120:701–713, 829–830.
3. Heijl A, Leske MC, Bengtsson B, Hyman L, Hussein M. Reduction of intraocular pressure and glaucoma progression: results from the Early Manifest Glaucoma Trial. *Arch Ophthalmol*. 2002;120:1268–1279.
4. Musch DC, Gillespie BW, Lichter PR, Niziol LM, Janz NK. Visual field progression in the Collaborative Initial Glaucoma Treatment Study: the impact of treatment and other baseline factors. *Ophthalmology*. 2009;116:200–207.
5. Collaborative Normal-Tension Glaucoma Study Group. The effectiveness of intraocular pressure reduction in the treatment of normal-tension glaucoma. *Am J Ophthalmol*. 1998;126:498–505.
6. Harris A, Sergott RC, Spaeth GL, Katz JL, Shoemaker JA, Martin BJ. Color Doppler analysis of ocular vessel blood velocity in normal-tension glaucoma. *Am J Ophthalmol*. 1994;118:642–649.

7. Broadway DC, Drance SM. Glaucoma and vasospasm. *Br J Ophthalmol*. 1998;82:862–870.
8. Sung KR, Cho JW, Lee S, et al. Characteristics of visual field progression in medically treated normal-tension glaucoma patients with unstable ocular perfusion pressure. *Invest Ophthalmol Vis Sci*. 2011;52:737–743.
9. Flammer J, Orgul S. Optic nerve blood-flow abnormalities in glaucoma. *Prog Retin Eye Res*. 1998;17:267–289.
10. Flammer J, Orgul S, Costa VP, et al. The impact of ocular blood flow in glaucoma. *Prog Retin Eye Res*. 2002;21:359–393.
11. Schmidl D, Garhofer G, Schmetterer L. The complex interaction between ocular perfusion pressure and ocular blood flow: relevance for glaucoma. *Exp Eye Res*. 2011;93:141–155.
12. Kaiser HJ, Schoetzau A, Stumpfig D, Flammer J. Blood-flow velocities of the extraocular vessels in patients with high-tension and normal-tension primary open-angle glaucoma. *Am J Ophthalmol*. 1997;123:320–327.
13. Grunwald JE, Piltz J, Hariprasad SM, DuPont J. Optic nerve and choroidal circulation in glaucoma. *Invest Ophthalmol Vis Sci*. 1998;39:2329–2336.
14. Gasser P, Flammer J. Blood-cell velocity in the nailfold capillaries of patients with normal-tension and high-tension glaucoma. *Am J Ophthalmol*. 1991;111:585–588.
15. Emre M, Orgul S, Gugleta K, Flammer J. Ocular blood flow alteration in glaucoma is related to systemic vascular dysregulation. *Br J Ophthalmol*. 2004;88:662–666.
16. Sugiyama T, Araie M, Riva CE, Schmetterer L, Orgul S. Use of laser speckle flowgraphy in ocular blood flow research. *Acta Ophthalmol*. 2010;88:723–729.
17. Aizawa N, Yokoyama Y, Chiba N, et al. Reproducibility of retinal circulation measurements obtained using laser speckle flowgraphy-NAVI in patients with glaucoma. *Clin Ophthalmol*. 2011;5:1171–1176.
18. Konishi NT, Kohra K, Fuji H. New laser speckle flowgraphy system using CCD camera. *Opt Rev*. 2002;9:163–169.
19. Watanabe G, Fujii H, Kishi S. Imaging of choroidal hemodynamics in eyes with polypoidal choroidal vasculopathy using laser speckle phenomenon. *Jpn J Ophthalmol*. 2008;52:175–181.
20. Wang L, Cull GA, Piper C, Burgoyne CF, Fortune B. Anterior and posterior optic nerve head blood flow in nonhuman primate experimental glaucoma model measured by laser speckle imaging technique and microsphere method. *Invest Ophthalmol Vis Sci*. 2012;53:8303–8309.
21. Takahashi H, Sugiyama T, Tokushige H, et al. Comparison of CCD-equipped laser speckle flowgraphy with hydrogen gas clearance method in the measurement of optic nerve head microcirculation in rabbits. *Exp Eye Res*. 2013;108:10–15.
22. Shiba T, Takahashi M, Hori Y, Maeno T. Pulse-wave analysis of optic nerve head circulation is significantly correlated with brachial–ankle pulse-wave velocity, carotid intima–media thickness, and age. *Graefes Arch Clin Exp Ophthalmol*. 2012;250:1275–1281.
23. Shiba T, Takahashi M, Hori Y, Maeno T, Shirai K. Optic nerve head circulation determined by pulse wave analysis is significantly correlated with cardio ankle vascular index, left ventricular diastolic function, and age. *J Atheroscler Thromb*. 2012;19:999–1005.
24. Zhou YQ, Faerestrand S, Matre K. Velocity distributions in the left ventricular outflow tract in patients with valvular aortic stenosis: effect on the measurement of aortic valve area by using the continuity equation. *Eur Heart J*. 1995;16:383–393.
25. Zhou YQ, Faerestrand S, Birkeland S, Matre K, Koller ME, Husby P. The velocity distribution in the aortic annulus at different times during systole is mainly determined by the pattern of flow convergence in the left ventricular outflow tract: an experimental study using Doppler colour flow mapping. *Clin Physiol*. 1995;15:597–610.
26. Zhou YQ, Abassi I, Faerestrand S. Flow velocity distributions in the left ventricular outflow tract and in the aortic annulus in patients with localized basal septal hypertrophy. *Eur Heart J*. 1996;17:1404–1412.
27. Sjoberg BJ, Eidenvall L, Loyd D, Wranne B, Ask P. Vascular characteristics influence the aortic ultrasound Doppler signal: computer and hydraulic model simulations. *Acta Physiol Scand*. 1993;147:271–279.
28. Crutchfield KE, Razumovsky AY, Tegeler CH, Mozayeni BR. Differentiating vascular pathophysiological states by objective analysis of flow dynamics. *J Neuroimaging*. 2004;14:97–107.
29. White CR, Haidekker M, Bao X, Frangos JA. Temporal gradients in shear, but not spatial gradients, stimulate endothelial cell proliferation. *Circulation*. 2001;103:2508–2513.
30. Hsiai TK, Cho SK, Honda HM, et al. Endothelial cell dynamics under pulsating flows: significance of high versus low shear stress slew rates (d(tau)/dt). *Ann Biomed Eng*. 2002;30:646–656.
31. Abegão Pinto L, Vandewalle E, De Clerck E, Marques-Neves C, Stalmans I. Ophthalmic artery Doppler waveform changes associated with increased damage in glaucoma patients. *Invest Ophthalmol Vis Sci*. 2012;53:2448–2453.
32. Kaeser P, Orgul S, Zawinka C, Reinhard G, Flammer J. Influence of change in body position on choroidal blood flow in normal subjects. *Br J Ophthalmol*. 2005;89:1302–1305.
33. Longo A, Geiser MH, Riva CE. Posture changes and subfoveal choroidal blood flow. *Invest Ophthalmol Vis Sci*. 2004;45:546–551.
34. Sayegh FN, Weigelin E. Functional ophthalmodynamometry: comparison between brachial and ophthalmic blood pressure in sitting and supine position. *Angiology*. 1983;34:176–182.
35. Riva CE, Grunwald JE, Petrig BL. Autoregulation of human retinal blood flow: an investigation with laser Doppler velocimetry. *Invest Ophthalmol Vis Sci*. 1986;27:1706–1712.
36. Tamaki Y, Araie M, Kawamoto E, Eguchi S, Fujii H. Non-contact, two-dimensional measurement of tissue circulation in choroid and optic nerve head using laser speckle phenomenon. *Exp Eye Res*. 1995;60:373–383.
37. Isono H, Kishi S, Kimura Y, Hagiwara N, Konishi N, Fujii H. Observation of choroidal circulation using index of erythrocytic velocity. *Arch Ophthalmol*. 2003;121:225–231.
38. Davies PF, Dewey CF Jr, Bussolari SR, Gordon EJ, Gimbrone MA Jr. Influence of hemodynamic forces on vascular endothelial function: in vitro studies of shear stress and pinocytosis in bovine aortic cells. *J Clin Invest*. 1984;73:1121–1129.
39. Ben Zekry S, Saad RM, Ozkan M, et al. Flow acceleration time and ratio of acceleration time to ejection time for prosthetic aortic valve function. *JACC Cardiovasc Imaging*. 2011;4:1161–1170.
40. Kuchan MJ, Jo H, Frangos JA. Role of G proteins in shear stress–mediated nitric oxide production by endothelial cells. *Am J Physiol*. 1994;267:C753–C758.
41. Frangos JA, Huang TY, Clark CB. Steady shear and step changes in shear stimulate endothelium via independent mechanisms: superposition of transient and sustained nitric oxide production. *Biochem Biophys Res Commun*. 1996;224:660–665.
42. Kezdi P, Stanley EL, Marshall WJ Jr, Kordenat RK. Aortic flow velocity and acceleration as an index of ventricular performance during myocardial infarction. *Am J Med Sci*. 1969;257:61–71.
43. Sainz A, Cabau J, Roberts VC. Deceleration vs. acceleration: a haemodynamic parameter in the assessment of vascular reactivity: a preliminary study. *Med Eng Phys*. 1995;17:91–95.
44. Cherecheanu AP, Garhofer G, Schmidl D, Werkmeister R, Schmetterer L. Ocular perfusion pressure and ocular blood flow in glaucoma. *Curr Opin Pharmacol*. 2013;13:36–42.

Investigative Ophthalmology & Visual Science

45. Resch H, Garhofer G, Fuchsjager-Mayrl G, Hommer A, Schmetterer L. Endothelial dysfunction in glaucoma. *Acta Ophthalmol*. 2009;87:4–12.
46. Galassi F, Sodi A, Ucci F, Renieri G, Pieri B, Baccini M. Ocular hemodynamics and glaucoma prognosis: a color Doppler imaging study. *Arch Ophthalmol*. 2003;121:1711–1715.
47. Crawford Downs J, Roberts MD, Sigal IA. Glaucomatous cupping of the lamina cribrosa: a review of the evidence for active progressive remodeling as a mechanism. *Exp Eye Res*. 2011;93:133–140.
48. Tezel G, Luo C, Yang X. Accelerated aging in glaucoma: immunohistochemical assessment of advanced glycation end products in the human retina and optic nerve head. *Invest Ophthalmol Vis Sci*. 2007;48:1201–1211.
49. Burgoyne CF. A biomechanical paradigm for axonal insult within the optic nerve head in aging and glaucoma. *Exp Eye Res*. 2011;93:120–132.
50. Zhou YQ, Faerestrand S, Matre K, Birkeland S. Velocity distributions in the left ventricular outflow tract and the aortic anulus measured with Doppler colour flow mapping in normal subjects. *Eur Heart J*. 1993;14:1179–1188.
51. Quigley HA, Vitale S. Models of open-angle glaucoma prevalence and incidence in the United States. *Invest Ophthalmol Vis Sci*. 1997;38:83–91.
52. Suzuki Y, Iwase A, Araie M, et al. Risk factors for open-angle glaucoma in a Japanese population: the Tajimi Study. *Ophthalmology*. 2006;113:1613–1617.
53. Gottanka J, Kuhlmann A, Scholz M, Johnson DH, Lutjen-Drecoll E. Pathophysiologic changes in the optic nerves of eyes with primary open angle and pseudoexfoliation glaucoma. *Invest Ophthalmol Vis Sci*. 2005;46:4170–4181.
54. Tamaki Y, Nagahara M, Araie M, Tomita K, Sandoh S, Tomidokoro A. Topical latanoprost and optic nerve head and retinal circulation in humans. *J Ocul Pharmacol Ther*. 2001; 17:403–411.
55. Makimoto Y, Sugiyama T, Kojima S, Azuma I. Long-term effect of topically applied isopropyl unoprostone on microcirculation in the human ocular fundus. *Jpn J Ophthalmol*. 2002;46: 31–35.
56. Tsuda S, Yokoyama Y, Chiba N, et al. Effect of topical tafluprost on optic nerve head blood flow in patients with myopic disc type. *J Glaucoma*. 2013;22:398–403.
57. Sugiyama T, Kojima S, Ishida O, Ikeda T. Changes in optic nerve head blood flow induced by the combined therapy of latanoprost and beta blockers. *Acta Ophthalmol*. 2009;87: 797–800.
58. Ohguro I, Ohguro H. The effects of a fixed combination of 0.5% timolol and 1% dorzolamide on optic nerve head blood circulation. *J Ocul Pharmacol Ther*. 2012;28:392–396.
59. Ishii K, Araie M. Effect of topical timolol on optic nerve head circulation in the cynomolgus monkey. *Jpn J Ophthalmol*. 2000;44:630–633.
60. Tamaki Y, Araie M, Muta K. Effect of topical dorzolamide on tissue circulation in the rabbit optic nerve head. *Jpn J Ophthalmol*. 1999;43:386–391.